

# A trade-off between ligand and strain effects optimizes the oxygen reduction activity of Pt alloys

## Supplementary Information

Regina M. Kluge,<sup>†a,\*</sup> Richard W. Haid,<sup>†a</sup> Alexander Riss,<sup>b</sup> Yang Bao,<sup>b</sup> Knud Seufert,<sup>b</sup> Thorsten O. Schmidt,<sup>a</sup> Sebastian A. Watzele,<sup>a</sup> Johannes V. Barth,<sup>b</sup> Francesco Allegretti,<sup>b</sup> Willi Auwärter,<sup>b</sup> Federico Calle-Vallejo,<sup>c,d,e,\*</sup> and Aliaksandr S. Bandarenka<sup>a,f,\*</sup>

### Table of Contents

S1.	Additional LT-STM images.....	2
S2.	Comparison of ORR activity data for Pt-Ni and Pt-Co alloy surfaces .....	3
S3.	Cu underpotential deposition and stripping curve .....	5
S4.	n-EC-STM technique and parameters.....	6
S5.	Additional n-EC-STM measurements .....	9
S6.	Additional computational details.....	12
S6.1.	Corrections and reaction pathway .....	12
S6.2.	Scaling relations .....	13
S6.3.	Assessing generalized coordination numbers on alloys.....	14
S6.4.	Predicting activity enhancements with respect to Pt(111) .....	16
S6.5.	Tabulated free energies and Cartesian coordinates .....	18
S7.	References .....	25

<sup>a</sup> Physik-Department ECS, Technische Universität München, James-Franck-Straße 1, 85748 Garching, Germany

<sup>b</sup> Physik-Department E20, Technische Universität München, James-Franck-Straße 1, 85748 Garching, Germany

<sup>c</sup> Nano–Bio Spectroscopy Group and European Theoretical Spectroscopy Facility (ETSF), Department of Polymers and Advanced Materials: Physics, Chemistry and Technology, University of the Basque Country UPV/EHU, Avenida Tolosa 72, 20018 San Sebastián, Spain.

<sup>d</sup> IKERBASQUE, Basque Foundation for Science, Plaza de Euskadi 5, 48009 Bilbao, Spain.

<sup>e</sup> Department of Materials Science and Chemical Physics & Institute of Theoretical and Computational Chemistry (IQTQUB), University of Barcelona, Martí i Franquès 1, 08028 Barcelona, Spain.

<sup>f</sup> Catalysis Research Center TUM, Ernst-Otto-Fischer-Straße 1, 85748 Garching, Germany.

## S1. Additional LT-STM images

The lattice constant in the main text was obtained from eight independent LT-STM measurements; an excerpt of those is given in Figure 1 and Figure S1. Per image, atomic distances were measured twice in each of the three directions of the crystal lattice (see arrows in Figure 1b). The calibration of the lateral scale was based on measurements of a Ag(111) surface. The statistical error of the final result was derived from the errors in both experiments, i.e., the measurements of the Pt<sub>3</sub>Ni(111) and Ag(111) surfaces. Systematic errors (due to small differences in the respective measurement temperatures, sample drift, piezo creep etc.) can additionally play a role. We have paid attention to minimising these errors in our experiments (e.g. by waiting for many hours for the samples to reach thermal equilibrium), but they cannot be completely eliminated. We estimate the statistical error on the order of a few per cent, which is less than the measured difference between the interatomic distances between Pt<sub>3</sub>Ni(111) and Pt(111). Therefore, we can conclude that compressive strain is present in the Pt<sub>3</sub>Ni(111) surface. In addition, these considerations explain the deviation between the experimentally determined lattice constant of Pt<sub>3</sub>Ni(111) and the one obtained from the DFT calculations.

In addition to the (111) lattice, we observe additional contrast at larger length scales, resembling an irregular superstructure. This contrast can be caused by (subsurface) defects/irregularities, as well as by small variations in the surface strain.

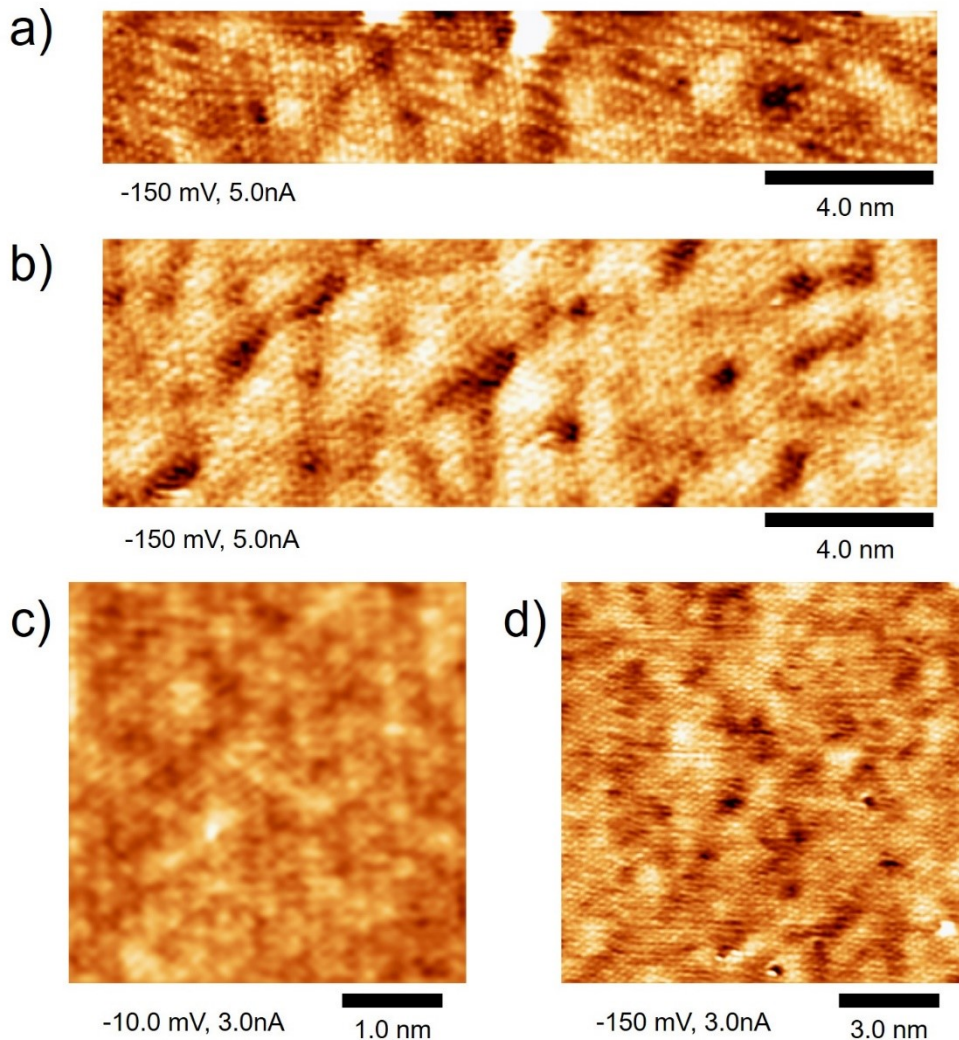


**Figure S1.** Additional LT-STM images. The tip-sample biases and tip current set-points are given under each image.

## S2. Comparison of ORR activity data for Pt-Ni and Pt-Co alloy surfaces

To recapitulate ORR activity trends on Pt-Ni and Pt-Co electrodes, the experimental result of this work is compared to the literature in Table S1. All experiments were done with an RDE setup, the conditions are specified in the table. The difference in activity between our work and reference [1] could be that the authors used a bead-type crystal while we used a disk-shaped one, or that our surface was prepared with a lower amount of defect sites, which would lower the overall activity according to this study. In the past, it was reported that  $\text{Pt}_3\text{Ni}(111)$  single crystal electrodes perform better than the other facets according to: (111) > (110) > (100).<sup>2</sup> The same trend was stated for  $\text{Pt}_3\text{Co}$  single-crystal model surfaces.<sup>3</sup> Macroscopic RDE experiments on stepped single crystals suggested that an increasing number

of (111) steps decreases the activity of  $\text{Pt}_3\text{Ni}(111)$  surfaces. In contrast,  $\text{Pt}[n(111) \times (100)]$  crystals outperform  $\text{Pt}(111)$  and showed an optimal performance between  $n = 3$  and  $n = 5$ . Therefore, sites at or close to (100) steps could be more active than (111) steps. By contrast, the same authors concluded for stepped  $\text{Pt}_3\text{Co}(111)$  single-crystal electrodes that the ORR activity increases with the increase of (111) and (100) step sites with optimal performances for  $\text{Pt}_3\text{Co}[3(111) \times (111)]$  and  $\text{Pt}_3\text{Co}[9(111) \times 100]$ .<sup>4</sup>

**Table S1.** Comparison of the ORR activity reported in this work on  $\text{Pt}_3\text{Ni}(111)$  with Pt-Ni, Pt-Co and Pt-Cu surfaces of other orientations from the literature. Note that the “ca.” stems from reading off the data of graphs and not from measurement uncertainties.

Material	Conditions	Activity @ 0.9 V <sub>RHE</sub>	References
$\text{Pt}_3\text{Ni}(111)$	room temperature, 1600 rpm rotational speed, $\text{O}_2$ -sat. 0.1 M $\text{HClO}_4$	7.6 mA cm <sup>-2</sup>	this work
$\text{Pt}_3\text{Ni}(111)$	room temperature, 1600 rpm rotational speed, $\text{O}_2$ -sat. 0.1 M $\text{HClO}_4$	ca. 3.2 mA cm <sup>-2</sup>	[1]
$\text{Pt}_3\text{Co}(111)$	room temperature, 1600 rpm rotational speed, $\text{O}_2$ -sat. 0.1 M $\text{HClO}_4$	ca. 2.7 mA cm <sup>-2</sup>	[4]
$\text{Pt}_x\text{Co}(111)$ $x = 27$ atom %	300 K temperature, 1500 rpm rotational speed, $\text{O}_2$ -sat. 0.1 M $\text{HClO}_4$	( $3.22 \pm 0.10$ ) mA cm <sup>-2</sup>	[3]
$\text{Pt}_3\text{Ni}(111)$	333 K temperature, 1600 rpm rotational speed, $\text{O}_2$ -sat. 0.1 M $\text{HClO}_4$	ca. 18 mA cm <sup>-2</sup>	[2]
$\text{Pt}_3\text{Ni}(110)$	333 K temperature, 1600 rpm rotational speed, $\text{O}_2$ -sat. 0.1 M $\text{HClO}_4$	ca. 5 mA cm <sup>-2</sup>	[2]
$\text{Pt}_3\text{Ni}(100)$	333 K temperature, 1600 rpm rotational speed, $\text{O}_2$ -sat. 0.1 M $\text{HClO}_4$	ca. 2 mA cm <sup>-2</sup>	[2]
$\text{Pt}_3\text{Ni}(\text{pc})$	333 K temperature, 1600 rpm rotational speed, $\text{O}_2$ -sat. 0.1 M $\text{HClO}_4$	ca. 3.3 mA cm <sup>-2</sup>	[5]
$\text{Pt}_3\text{Co}(\text{pc})$	333 K temperature, 1600 rpm rotational speed, $\text{O}_2$ -sat. 0.1 M $\text{HClO}_4$	ca. 4.4 mA cm <sup>-2</sup>	[5]
Pt-Cu NSAs	60 °C temperature, 1600 rpm rotational speed, $\text{O}_2$ -sat. 0.1 M $\text{HClO}_4$	ca. 7.6 mA cm <sup>-2</sup>	[6]

### S3. Cu underpotential deposition and stripping curve

The electrochemically active surface area was determined using Cu underpotential deposition (UPD) and subsequent stripping.<sup>7,8</sup> For this purpose, 0.1 M CuO (99.999%, Merck KGaA, Germany) was first dissolved in a solution of 0.3 M HClO<sub>4</sub>. Subsequently, the mixture was stirred overnight until a bright blue, homogenous solution was obtained. Then, the solution was diluted to a concentration of 3.33 mM Cu<sup>2+</sup> in 0.1 M HClO<sub>4</sub>. The electrode was employed in the cell in a hanging meniscus configuration and, at first, cycled between 0.4 V<sub>RHE</sub> and 1.0 V<sub>RHE</sub> for approx. 10 repetitions to ensure a stable voltammogram, then held at 1.0 V<sub>RHE</sub> to exclude Cu on the surface. For the Cu UPD experiment, the electrode was held at 0.4 V<sub>RHE</sub> for 3 min and then swept to a potential of 1.0 V<sub>RHE</sub> at a rate of 50 mV s<sup>-1</sup>. The corresponding curve is given in Figure S2. The area of the Cu UPD peak is approximately 455  $\mu\text{C cm}^{-2}$ . It is larger than for pure Pt (440  $\mu\text{C cm}^{-2}$ ).<sup>7,8</sup> Since the experiment was done after the EC-STM measurements, a possible reason for the slight increase of the surface area could be roughening due to cycling in an acidic medium. This is an indicator that the surface is indeed only comprised of Pt and that Ni is leached out.

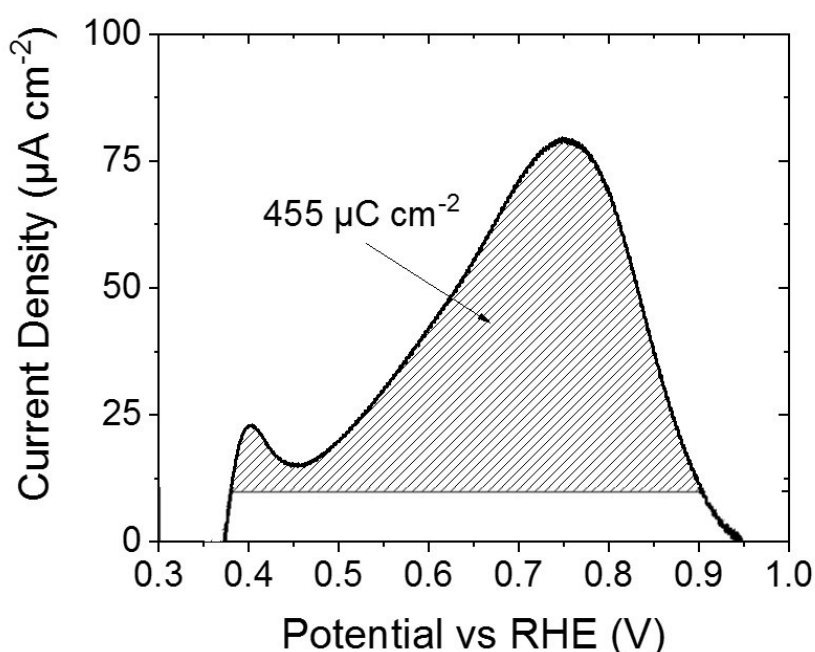


**Figure S2.** Typical anodic sweep for stripping off the underpotentially deposited Cu monolayer from Pt<sub>3</sub>Ni(111) after the electrochemical experiments. Experimental details are given in the text above this figure.

#### S4. n-EC-STM technique and parameters

Comparing the data when the reaction is “on” and “off”, the STM signal in the former case is destabilized and shows an increased noise level compared to the latter. When the reaction is turned “on”, the noise level is increased when the tip is scanning over an active site. In the sketch in Figure S3 a and b, some surface atoms are exemplarily assigned as “active” and coloured in yellow. At these positions, a significant increase in the noise level of the recorded signal can be observed, as depicted in the inset.

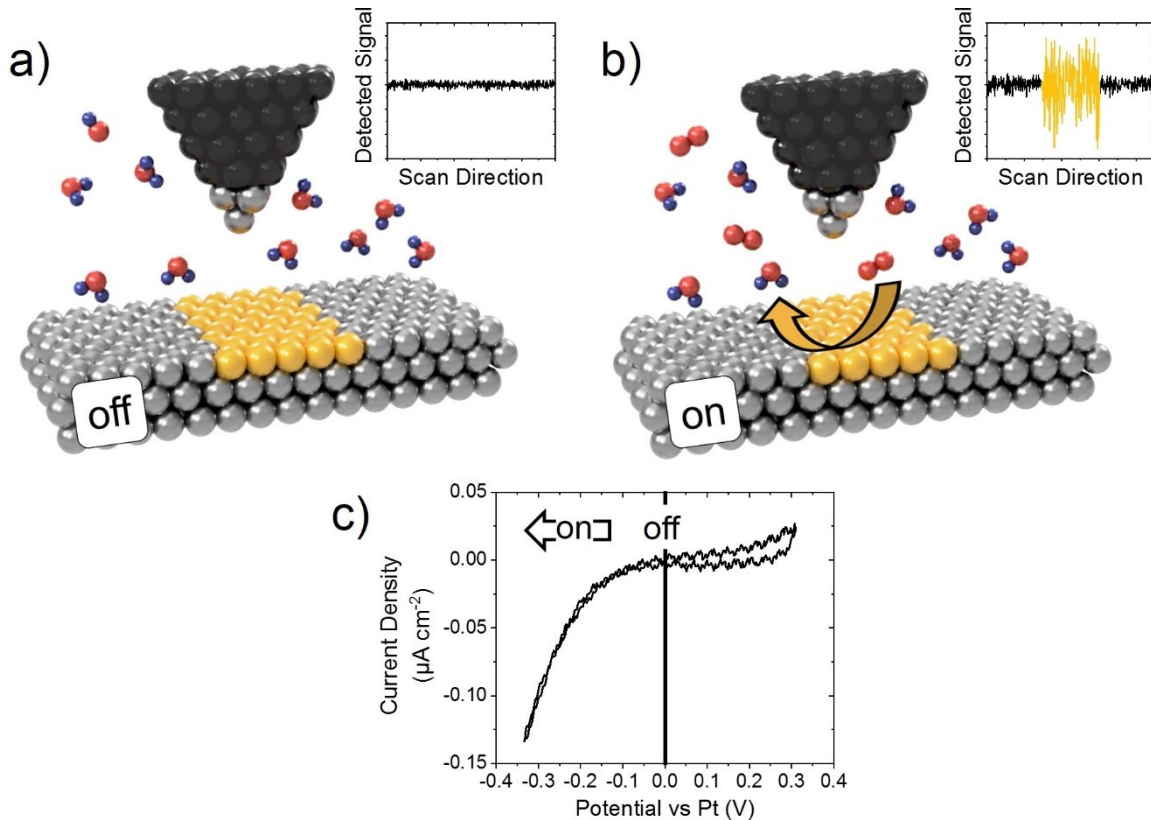


**Figure S3.** a,b) Schematics of an n-EC-STM measurement. A destabilisation of the STM signal can be observed when the reaction is turned “on” (b) compared to “off” (a). The most prominent increase in the noise level occurs when the tip is placed over the active sites, allowing for their identification. Colour code: sample (silver), active sites (yellow), oxygen (red), hydrogen (blue). c) CV recorded in EC-STM setup against a Pt *quasi*-reference electrode. For all measurements, a potential of 0 mV<sub>Pt</sub> was assigned to reaction “off”, and a negative potential to reaction “on”. Details of the measurement parameters on Pt<sub>3</sub>Ni(111) are given in Table S2.

An example of the high resolution of the n-EC-STM measurements is given in Figure S4. Here, the step sites distinctly show an increase in the noise level over adjacent terrace sites for Pt(111) in 0.1 M HClO<sub>4</sub> under ORR conditions. In the paper, besides the high resolution, a direct quantitative relation between noise level and ORR activity was proven. For further reading, please see ref. [9]. In the past, the n-EC-STM technique was used to identify active terraces of polycrystalline Pt alloys for the ORR.<sup>10</sup> However, we resorted to a well-defined single-crystalline model system for this study to be able to extract more valuable information. As a side note, there are other systems where terrace and step sites show comparable activities and noise levels, which was in that particular case attributed to their amorphous nature.<sup>11</sup>

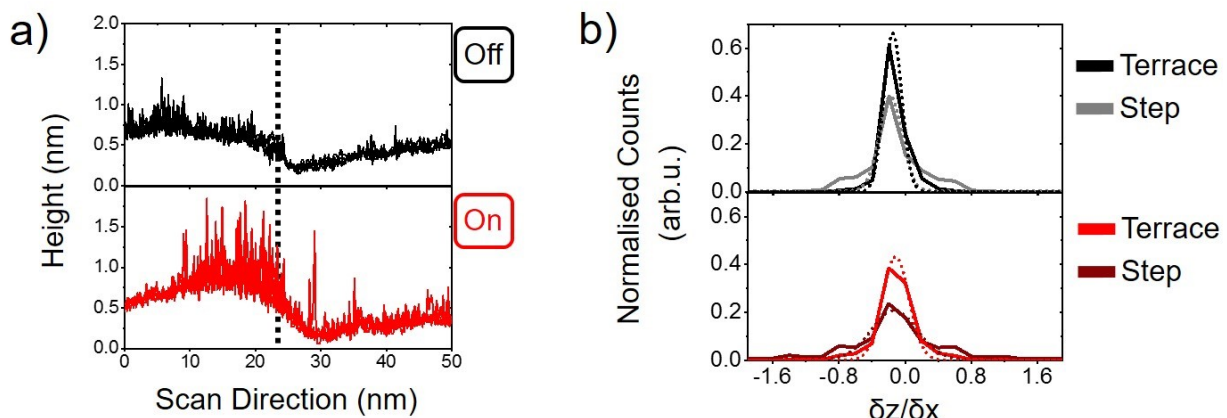


**Figure S4.** a) Typical EC-STM measurement on Pt(111) in 0.1 M HClO<sub>4</sub> under ORR conditions. Under reaction conditions, “on” (red curve), the step sites exhibit a higher noise level than the adjacent terrace site. b) Corresponding histograms of the signal derivatives, see main text of manuscript for definition. Under reaction conditions, the histogram of the step site shows a lower intensity and broader texture, confirming the higher noise level. Data taken from ref. [9]. © 2020 The Authors. Published by Wiley-VCH GmbH.

**Table S2.** Experimental parameters of each n-EC-STM image presented in this work.

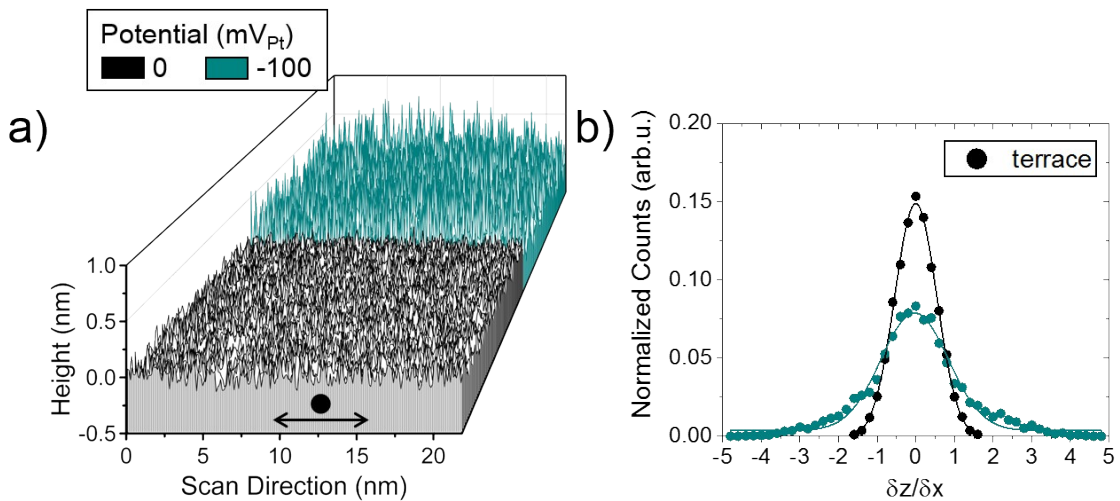
figure number	sample potential “on” (mV <sub>Pt</sub> )	tip potential (mV <sub>Pt</sub> )	current set-point (nA)
Figure 2		-100	-30
Figure 3/Figure S6	as marked in the image		-50
Figure S5		-100	-20
Figure S7	as marked in the image		-50

**Table S3.** Parameters obtained in the fits of the histograms of all n-EC-STM images presented in the main text and this Supporting Information. Symbols refer to: ● – terrace site; ♦ – step.

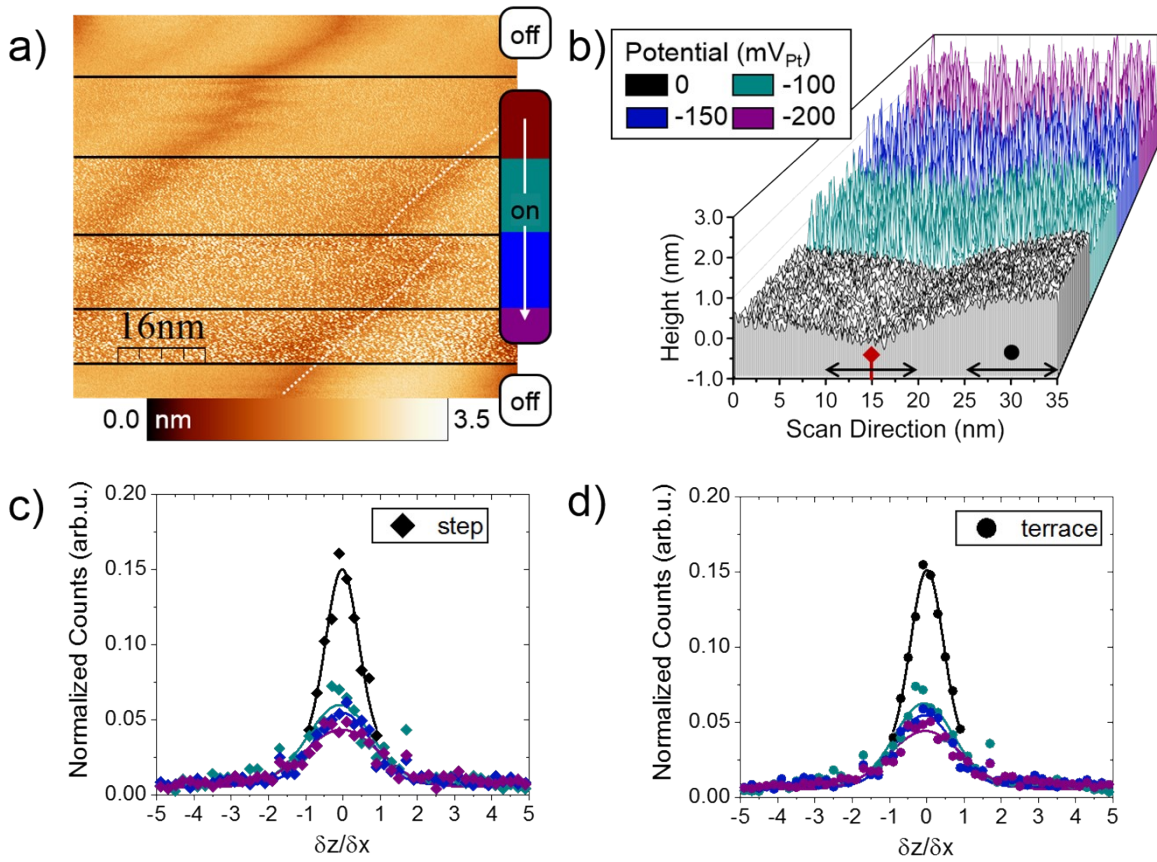
figure number		potential (mV <sub>pt</sub> )	FWHM	FWHM	height	height	reduced chi-square	r-square
			value	error	value	error		
Figure 2	♦	0	0.43	0.0035	0.44	0.0028	3.8E-06	1.00
	●	0	0.44	0.013	0.43	0.0091	4.3E-05	1.00
	♦	- 100	1.1	0.031	0.14	0.0031	2.6E-05	0.99
	●	- 100	1.3	0.042	0.11	0.0028	2.4E-05	0.98
Figure 3	♦	0	1.2	0.22	0.13	0.023	6.2E-05	0.96
	●	0	1.5	0.40	0.16	0.051	5.5E-05	0.96
	♦	-50	1.6	0.11	0.10	0.0044	4.2E-05	0.97
	●	-50	1.6	0.11	0.091	0.0043	4.1E-05	0.96
	♦	-100	1.8	0.088	0.051	0.0021	1.8E-05	0.94
	●	-100	1.9	0.082	0.050	0.0020	1.6E-05	0.94
	♦	-150	2.1	0.13	0.041	0.0022	2.4E-05	0.84
	●	-150	2.1	0.12	0.041	0.0019	1.9E-05	0.87
Figure S5	●	0	1.3	0.025	0.15	0.0020	8.0E-06	1.00
	●	-100	2.0	0.061	0.075	0.0018	1.5E-05	0.98
Figure S6	♦	0	1.0	0.19	0.12	0.017	1.1E-04	0.93
	●	0	1.0	0.093	0.12	0.0084	2.7E-05	0.98
	♦	-100	1.9	0.15	0.052	0.0033	5.1E-05	0.84
	●	-100	2.0	0.12	0.055	0.0030	3.9E-05	0.88
	♦	-150	1.8	0.10	0.048	0.0022	2.2E-05	0.88
	●	-150	1.8	0.10	0.048	0.0021	2.0E-05	0.89
	♦	-200	2.3	0.12	0.039	0.0017	1.6E-05	0.87
	●	-200	2.4	0.13	0.038	0.0018	1.8E-05	0.86

Figure S7			-25	1.16	0.04	0.16	0.004	3.5E-05	0.99
	◆	-25	1.2	0.039	0.15	0.0036	3.1E-05	0.99	
	●	-50	0.98	0.037	0.16	0.0050	5.9E-05	0.98	
	●	-50	1.1	0.036	0.14	0.0038	3.6E-05	0.98	
	◆	-100	1.3	0.029	0.12	0.0022	1.5E-05	0.99	
	●	-100	1.4	0.028	0.10	0.0018	1.0E-05	0.99	
	◆	-150	0.78	0.012	0.21	0.0028	1.4E-05	0.99	
	●	-150	0.89	0.025	0.14	0.0033	2.3E-05	0.97	
	◆	-200	1.3	0.035	0.10	0.0023	1.6E-05	0.98	
	●	-200	1.4	0.047	0.081	0.0023	1.8E-05	0.95	

## S5. Additional n-EC-STM measurements



**Figure S5.** a) n-EC-STM measurement on a Pt<sub>3</sub>Ni(111) terrace in 0.1 M HClO<sub>4</sub>. Note that the diameter of one Pt atom is ca. 0.27 nm. The STM signal is noisier when the reaction is switched “on” (green, -100 mV<sub>Pt</sub>) compared to “off” (black, 0 mV<sub>Pt</sub>). b) Histograms of the signal derived with respect to adjacent data points as described in the main text. The histogram broadens and loses intensity if the reaction is switched “on”. The dataset for the histograms is the area marked with an arrow in (a).



**Figure S6.** a) Same STM image as Figure 3 in the main text. Here, the step edge on the right is evaluated. b) Waterfall plot of the step edge on the right marked in (a). c,d) Histograms rendered from the step and terrace sites, respectively. Data were taken as marked in the waterfall plot in (b).

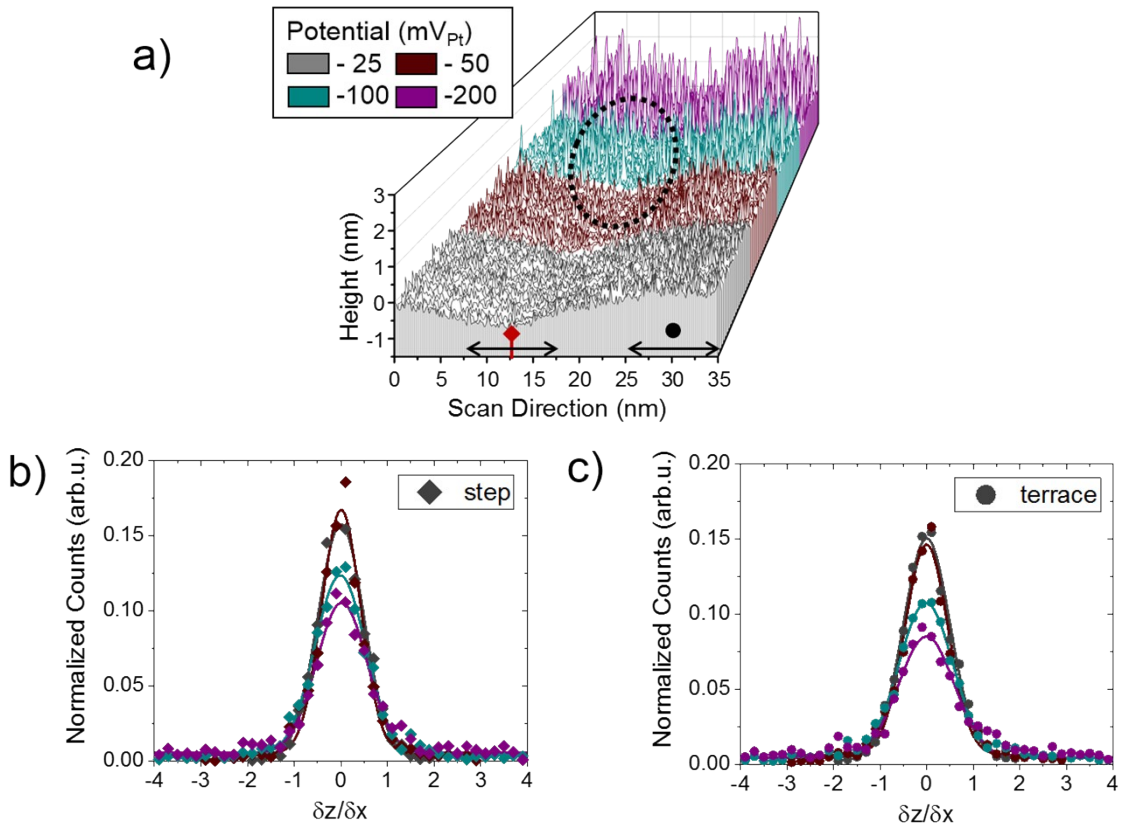


**Figure S7.** a) Additional n-EC-STM measurement across a step edge when applying different potentials as labelled by the colour code. The noise level near the bottom of the step is less distinct than at terrace sites (e.g. at the position encircled in black) when the reaction is “on”. b,c) Histograms for step and terrace sites, respectively. Step sites show lower FWHMs than terrace sites at each potential step (c.f. Table S3), which indicates their lower activity.

## S6. Additional computational details

### S6.1. Corrections and reaction pathway

Table S4 contains the zero-point energies (ZPE) and entropy (TS) corrections of the gases, liquids and adsorbates needed to model the ORR. All values are in eV; T = 298.15 K.

**Table S4.** ZPE and TS corrections for gases, liquids and adsorbates in this study.

species	ZPE (eV)	TS (eV)
H <sub>2</sub> (g)	0.27	0.40
H <sub>2</sub> O(l)	0.57	0.67
*OH	0.33	–
*OOH	0.43	–

The adsorbate-solvent stabilization corrections for \*OH on pure Pt, Pt<sub>3</sub>Cu, Pt<sub>3</sub>Ni, Pt<sub>3</sub>Co, and Pt<sub>3</sub>Ti were -0.58, -0.56, -0.53, -0.56 eV, and -0.55 eV, respectively. The values for Pt were taken from previous works,<sup>12</sup> while those for Pt<sub>3</sub>M were calculated following the method therein. The values for PtCu NSAs were calculated as the arithmetic average of Pt and PtCu NSAs with 1 ML Cu reported previously and were -0.56, -0.52 and -0.47 eV for 0.25, 0.50 and 0.75 ML Cu in the subsurface, respectively.<sup>12</sup>

The associative ORR pathway in acid is taken from the seminal work of Nørskov and co-workers<sup>13</sup> and is given by Equations S1-4. This pathway is known to have lower kinetic barriers than the dissociative pathway on Pt-based materials.<sup>14</sup>



Energetically, the pathway can be expressed in terms of the free energies of adsorption of \*O, \*OH and \*OOH, as shown in Equations S5-8:

$$\Delta G_1 = \Delta G_{OOH} - \Delta G_{O_2} \quad (S5)$$

$$\Delta G_2 = \Delta G_O - \Delta G_{OOH} \quad (S6)$$

$$\Delta G_3 = \Delta G_{OH} - \Delta G_O \quad (S7)$$

$$\Delta G_4 = \Delta G_{H_2O} - \Delta G_{OH} \quad (S8)$$

where  $\Delta G_{H_2O} = 0$  and  $\Delta G_{O_2} = 4.92$  eV. The potential-limiting steps for most catalysts correspond to Equations (1) and (4), for weak and strong binding, respectively.

## S6.2. Scaling relations

The scaling relation between the adsorption energies of \*OH and \*OOH on pure Pt surfaces is provided in Figure S8, using data from previous works.<sup>15</sup> Furthermore, the vertical separation (that is, assuming that the slope of the fit is 1, which entails an MAE of 0.02 eV and a MAX of 0.05 eV, similar to those in Figure S8) between the energies is 3.12 eV on average, which was used to approximate the \*OOH adsorption energies of the alloys.

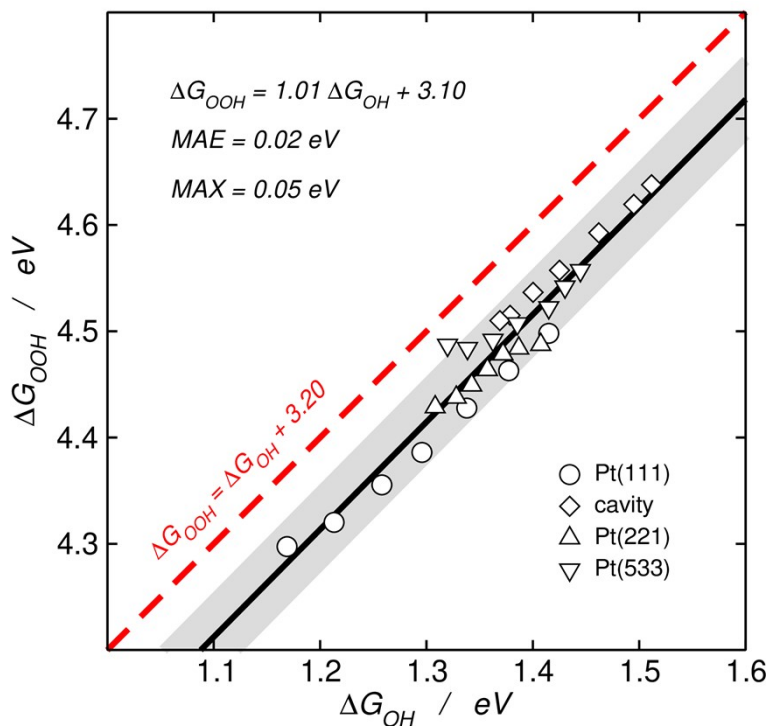


**Figure S8.** Adsorption-energy scaling relation between \*OOH and \*OH on pure Pt sites. The equation of the linear is given together with its associated mean and maximum absolute errors (MAE, MAX). The conventional scaling relation with a unity slope and an offset of 3.2 eV is provided in red for comparison.

### S6.3. Assessing generalized coordination numbers on alloys

Using the linear relationship found in Figure 4a in the main text for pure Pt sites ( $\Delta E_{OH} = 0.21 \overline{CN}^* - 0.62$ ), it is possible to estimate  $\overline{CN}^*$  for alloy sites since all analysed surfaces have a Pt skin and \*OH is always bound to Pt. Since the  $\overline{CN}^*$  of an analogous site on pure Pt is known, it is possible to calculate the equivalence of an M atom (M = Cu, Ni, Co, Ti) neighbour in terms of Pt neighbours ( $n_M$ ), see Table S5.

**Table S5.** Assessment of generalized coordination numbers on  $Pt_3M$  (M = Cu, Ni, Co, Ti). T: terrace, B: step bottom, SE: step edge, AD: Pt adatom. M: Ni or Co. The last column indicates the equivalence of an M atom in terms of Pt nearest neighbours. The ranges provided for the average  $n_M$  contain at least 85% of the data.

site	$\Delta E_{OH}$ / eV	$\overline{CN}^*$	$\overline{CN}^* @ Pt$	$n_M$
$Pt_3Cu(111)$ -T	1.15	8.28	7.50	1.78
$Pt_3Cu(533)$ -B	1.14	8.26	7.67	1.59
$Pt_3Cu(533)$ -SE	0.70	6.16	5.50	1.66
$Pt_3Cu(533)$ -T	1.15	8.29	7.50	1.79
		average	1.70 ± 0.12	
$Pt_3Ni(111)$ -T	1.10	8.05	7.50	1.55
$Pt_3Ni(221)$ -B	1.16	8.32	7.83	1.49
$Pt_3Ni(221)$ -SE	0.75	6.43	5.50	1.93
$Pt_3Ni(533)$ -B	1.13	8.20	7.67	1.53
$Pt_3Ni(533)$ -SE	0.65	5.96	5.50	1.46
1AD @ $Pt_3Ni(111)$	0.03	3.01	2.50	1.34
2AD @ $Pt_3Ni(111)$	0.29	4.24	3.50	1.81
		average	1.59 ± 0.25	
$Pt_3Co(111)$ -T	1.07	7.92	7.50	1.42
$Pt_3Co(533)$ -B	1.13	8.20	7.67	1.53
$Pt_3Co(533)$ -SE	0.66	5.98	5.50	1.48
$Pt_3Co(533)$ -T	1.08	7.97	7.50	1.47
		average	1.48 ± 0.05	
$Pt_3Ti(111)$ -T	1.05	7.82	7.50	1.32
$Pt_3Ti(533)$ -B	1.14	8.26	7.67	1.59
$Pt_3Ti(533)$ -SE	0.65	5.94	5.50	1.44
$Pt_3Ti(533)$ -T	1.05	7.84	7.50	1.34
		average	1.42 ± 0.17	

For instance, consider  $Pt_3Ni(111)$ -T sites, the \*OH adsorption energy of which is 1.10 eV. The corresponding generalized coordination number is 8.05, which is 0.55 units larger than that of  $Pt(111)$ -T. Such sites have 9 nearest neighbours: 6 in the surface layer (with  $cn = 9$ ) and

3 in the subsurface layer (with  $cn = 12$ ). Since the Ni neighbour is in the subsurface, we have that:  $8.05 = (6 \times 9 + 2 \times 12 + n_{Ni} \times 12)/12$ . Thus,  $n_{Ni} = 1.55$ .

The analysis is similar for PtCu(111) near-surface alloys. Table S6 shows the adsorption energies of \*OH depending on the Cu content and the number of Cu neighbours of the active sites. In turn, Table S7 displays the values of  $n_{Cu}$ . Briefly, 1 Cu neighbour at an unstrained PtCu(111) NSA is on average equivalent to 1.08 Pt neighbours; when there are 2 Cu neighbours, each of them counts as 1.29 Pt neighbours; and when there are 3 Cu neighbours, each of them is equivalent to 1.52 Pt neighbours.

**Table S6.**  $\Delta E_{OH}$  (in eV) as a function of the number of Cu neighbours in the subsurface and the total coverage of Cu ( $\theta_{Cu}$  in ML).

$\theta_{Cu}$	subsurface neighbours		
	1 Cu	2 Cu	3 Cu
0.25	0.98	-	-
0.50	1.02	1.08	-
0.75	-	1.14	1.34
1.00	-	-	1.30
average	1.00	1.11	1.32

**Table S7.** Values of  $n_{Cu}$  as a function of the number of Cu neighbours in the subsurface and the total coverage of Cu ( $\theta_{Cu}$  in ML).

$\theta_{Cu}$	subsurface neighbours		
	1 Cu	2 Cu	3 Cu
0.25	1.00	-	-
0.50	1.15	1.22	-
0.75	-	1.36	1.55
1.00	-	-	1.49
average	1.08	1.29	1.52

We note that the generalized coordination formula for an atom  $i$  in with a total of  $n$

nearest neighbours the coordination number of which is  $cn(j)$ :  $CN(i) = \sum_{j=1}^n cn(j)/cn_{max}$ . In this equation,  $cn_{max}$  is the maximum number of nearest neighbours in the bulk. The maximum generalized coordination number ( $CN(i)_{max}$ ) is found in the limit in atom  $i$  has  $n = n_{max}$  neighbours and their coordination is  $cn(j) = cn_{max}$ . In view of this,  $CN(i)_{max} = n_{max}$ . For an fcc

crystal,  $n_{max} = 12$ . In sum, the maximum generalized coordination number is 12, which coincides with the maximum conventional coordination number.

The assessment of the  $\bar{CN}^*$  that represents an entire catalyst in Figure 4c is detailed in the next subsection.

#### S6.4. Predicting activity enhancements with respect to Pt(111)

In the following, we will assume that: (i) the current density is the sum of the individual current densities of the active sites, (ii) the symmetry factors ( $\beta$ ) are identical for pure Pt and Pt alloys and equal to the usual value of 0.5,<sup>16</sup> and (iii) the number of active sites per unit cell and the preexponential factors are the same for pure Pt and Pt alloys. A simplified version of the Butler-Volmer equation for Pt(111) and a given electrocatalyst  $m$  is the following:

$$j_{Pt(111)} = \frac{I_{Pt(111)}}{A_{Pt(111)}} = \frac{\sum e^{\beta\eta_i/k_B T}}{A_{Pt(111)}} \quad (S9)$$

$$j_m = \frac{I_m}{A_m} = \frac{\sum e^{\beta\eta_m/k_B T}}{A_m} \quad (S10)$$

where  $j$  is the current density,  $I$  the current,  $k_B$  the Boltzmann constant,  $A$  the surface area,  $T$  the absolute temperature, and  $\eta = U - U_0$  the overpotential. The activity enhancement (AE) with respect to Pt(111) is:

$$AE = \ln\left(\frac{j_m}{j_{Pt(111)}}\right) = \ln\left(\frac{\sum e^{\beta\eta_i/k_B T}}{\sum e^{\beta\eta_m/k_B T}}\right) + \ln\left(\frac{A_{Pt(111)}}{A_m}\right) \quad (S11)$$

If all sites on Pt(111) are identical and there are  $N$  of them in  $A_{Pt(111)}$ , it can be shown that the activity enhancement is:

$$AE = \ln\left(\sum e^{\beta[U_m - U_{Pt(111)}]/k_B T}\right) + \ln\left(\frac{A_{Pt(111)}}{N_{Pt(111)} A_m}\right) \quad (S12)$$

Equation S12 was used to make Figure 4c. We used 2×2 (111) slabs (so that  $N_{Pt(111)} = 4$ ), 1×2 (533) slabs and 1×2 (221) slabs. The corresponding areas can be found in Table S8.

**Table S8.** Geometric areas (in Å<sup>2</sup>) of the catalysts under study.

Catalyst	A <sub>111</sub>	A <sub>533</sub>	A <sub>221</sub>
Pt	6.85	21.60	21.60
Pt <sub>3</sub> Cu	6.60	20.81	20.81
Pt <sub>3</sub> Ni	6.53	20.60	20.60
Pt <sub>3</sub> Co	6.56	20.68	20.68
Pt <sub>3</sub> Ti	6.75	21.30	21.30

The values of  $\overline{CN}^*$  that represent an entire catalyst in Figure 4c are obtained as a Boltzmann-like average depending on the activity of the sites, as shown in Equation S13.

$$\overline{CN}_{Pt_3M}^* = \frac{\sum \overline{CN}_m * \cdot e^{\beta U_m / k_B T}}{\sum e^{\beta U_m / k_B T}} \quad (S13)$$

### S6.5. Tabulated free energies and Cartesian coordinates

In Table S9, we provide a list of the pure Pt sites included in Figure 4a together with their generalized coordination numbers and \*OH binding energies.

**Table S9.** Generalized coordination and \*OH binding energies of pure Pt sites. B: step bottom, SE: step edge, s: strain in % (negative when compressing, positive when expanding).

Site	$\overline{CN}^*$	$\Delta E_{OH}$ / eV
Pt(111)	s = -3.00%	7.73
	s = -2.00%	7.65
	s = -1.00%	7.58
	s = 0.00%	7.50
	s = 1.00%	7.43
	s = 2.00%	7.35
	s = 3.00%	7.28
	s = -3.00%	8.08
	s = -2.00%	7.99
Pt(221)	s = -1.00%	7.91
	s = 0.00%	7.83
	s = 1.00%	7.76
	s = 2.00%	7.68
	s = 3.00%	7.61
	s = -3.00%	8.25
	s = -2.00%	8.16
	s = -1.00%	8.08
	s = 0.00%	8.00
cavity	s = 1.00%	7.92
	s = 2.00%	7.84
	s = 3.00%	7.77
	s = -3.00%	7.90
	s = -2.00%	7.82
	s = -1.00%	7.74
	s = 0.00%	7.67
	s = 1.00%	7.59
	s = 2.00%	7.52
Pt(533)	s = 3.00%	7.44
	Pt(100)	6.67
	Pt(110)	5.83
	Pt(221)-SE	5.50
	Pt(533)-SE	5.50
	s-Pt(111)	7.68
	s-Pt(221)-B	8.02
	s-Pt(533)-B	7.85
	s-Pt(221)-SE	5.63
Pt AD @ Pt(111)	s-Pt(533)-SE	5.63
	Pt AD @ Pt(111)	2.50
	s-Pt AD @ Pt(111)	2.56
	2AD @ Pt(111)	3.50
	s-2AD @ Pt(111)	3.58

In Table S10, we provide a list of the sites at strained Pt surfaces and Pt alloys. Because of the scale, some data points do not appear in Figure 4b. The generalized coordination numbers and ORR limiting potentials are provided in each case.

**Table S10.** Generalized coordination and limiting potentials of sites at strained Pt surfaces and Pt alloys. B: step bottom, ML: monolayers, NN: nearest neighbours, SE: step edge, s: strain in % (negative when compressing, positive when expanding), T: terrace. Note: -2.31, -2.14, -1.84 and -0.68% are the strain percentages in  $\text{Pt}_3\text{Ni}$ ,  $\text{Pt}_3\text{Co}$ ,  $\text{Pt}_3\text{Cu}$ , and  $\text{Pt}_3\text{Ti}$ , respectively.

Site	$\bar{CN}^*$	$\Delta U / V$
Pt(111)	7.50	0.72
s-Pt(111) (s = -2.31%)	7.68	0.79
s-Pt(111) (s = -2.14%)	7.66	0.79
s-Pt(111) (s = -1.84%)	7.64	0.77
s-Pt(111) (s = -0.68%)	7.55	0.75
s-Pt(221)-B (s = -2.31%)	8.02	0.81
s-Pt(533)-B (s = -2.31%)	7.85	0.85
s-Pt(221)-SE (s = -2.31%)	5.63	0.34
s-Pt(533)-SE (s = -2.31%)	5.63	0.32
s-Pt(221)-T (s = -2.31%)	7.68	0.83
s-Pt(533)-T (s = -2.31%)	7.68	0.84
$\text{Pt}_3\text{Ni}(111)$ -T	8.05	0.86
$\text{Pt}_3\text{Ni}$ (221)-B	8.32	0.81
$\text{Pt}_3\text{Ni}$ (221)-SE	6.43	0.55
$\text{Pt}_3\text{Ni}$ (221)-T	8.06	0.86
$\text{Pt}_3\text{Ni}$ (533)-B	8.20	0.83
$\text{Pt}_3\text{Ni}$ (533)-SE	5.98	0.46
$\text{Pt}_3\text{Ni}$ (533)-T	7.98	0.84
AD @ $\text{Pt}_3\text{Ni}(111)$	3.01	-0.17
2AD @ $\text{Pt}_3\text{Ni}(111)$	4.24	0.09
$\text{Pt}_3\text{Co}(111)$ -T	7.92	0.84
$\text{Pt}_3\text{Co}(533)$ -B	8.20	0.83
$\text{Pt}_3\text{Co}(533)$ -SE	5.98	0.43
$\text{Pt}_3\text{Co}(533)$ -T	7.97	0.85
$\text{PtCu}(111)$ 0.25 ML (1 Cu NN)	7.58	0.75
$\text{PtCu}(111)$ 0.25 ML (0 Cu NN)	7.50	0.72
$\text{PtCu}(111)$ 0.5 ML (2 Cu NN)	8.09	0.89
$\text{PtCu}(111)$ 0.5 ML (1 Cu NN)	7.58	0.83
$\text{PtCu}(111)$ 0.75 ML (2 Cu NN)	8.09	0.83
$\text{PtCu}(111)$ 0.75 ML (3 Cu NN)	9.07	0.63
$\text{Pt}_3\text{Cu}(111)$ -T	8.28	0.81
$\text{Pt}_3\text{Cu}(533)$ -B	8.26	0.82
$\text{Pt}_3\text{Cu}(533)$ -SE	6.16	0.47
$\text{Pt}_3\text{Cu}(533)$ -T	8.29	0.81
$\text{Pt}_3\text{Ti}(111)$ -T	7.82	0.83
$\text{Pt}_3\text{Ti}(533)$ -B	8.26	0.82
$\text{Pt}_3\text{Ti}(533)$ -SE	5.94	0.43
$\text{Pt}_3\text{Ti}(533)$ -T	7.84	0.83

In Table S11, we provide a list of the catalysts together with the Boltzmann-weighted generalized coordination numbers and ORR activity enhancements with respect to Pt(111).

**Table S11.** Electrocatalytic activity enhancement (AE) with respect to Pt(111).

catalyst	average $\overline{CN}^*$	$0.72 AE_{DFT}$	$AE_{exp}$	references for $AE_{exp}$
Pt <sub>3</sub> Co(111)	7.90	1.66	1.45	[4]
Pt <sub>3</sub> Co(533)	7.95	1.59	1.60	[4]
Pt <sub>3</sub> Ni(111)	8.02	1.95	1.68, 2.10	[1, 17]
Pt <sub>3</sub> Ni(533)	7.91	1.45	-	
Pt <sub>3</sub> Ni(221)	8.00	1.31	1.45	[1]
PtCu 0.25 ML	7.57	0.46	0.74	[6]
PtCu 0.50 ML	7.96	2.08	2.08	[6]
PtCu 0.75 ML	8.09	1.86	-	
Pt <sub>3</sub> Cu(111)	8.19	1.82	-	
Pt <sub>3</sub> Cu(533)	8.08	1.87	-	
Pt <sub>3</sub> Ti(111)	7.81	2.03	-	
Pt <sub>3</sub> Ti(533)	7.93	1.71	-	
Pt(533)	7.62	0.72	0.74	[18]

Figure S9 shows the location of the terrace, step edge and step bottom sites at (111), (221) and (533) model surfaces.

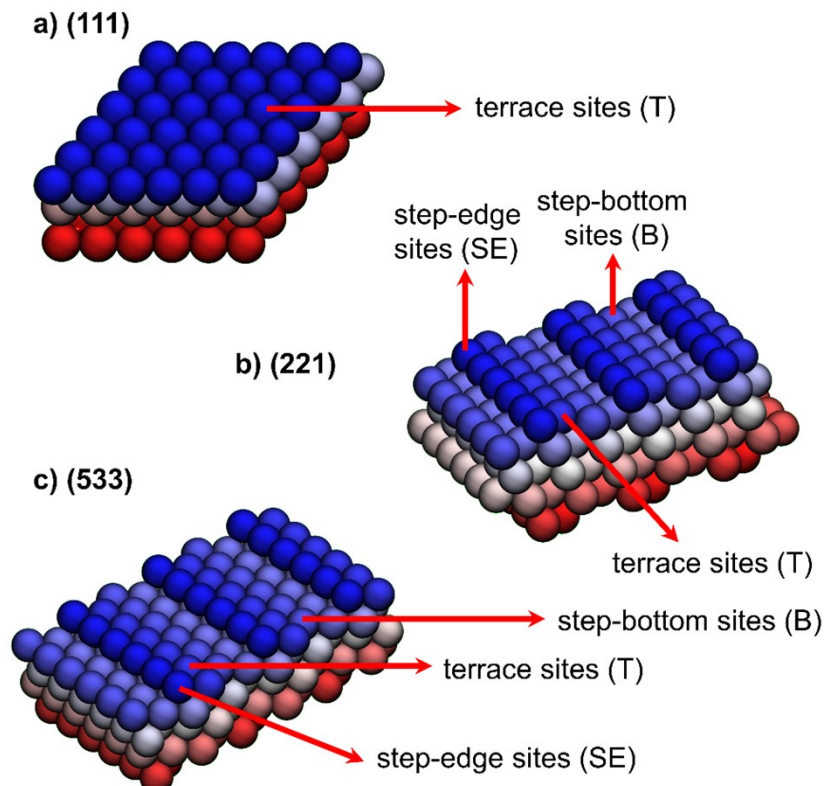


**Figure S9.** Sites at a) (111), b) (221), and c) (533) surfaces.

In the following, we provide the CONTCAR files for the active sites in this study.

Pt3Co111	0.5585220201102440 0.7637670814744445 0.9388310524722919 TTT	0.7499996358617906 0.5000004204710535 0.731127600000007 FFF
1.0000000000000000	0.7473660870187592 0.0244325450700865 0.9137226505489899 TTT	0.0036933218964636 -0.0122283000640023 0.0865866450179126 TTT
5.5025100000000000	0.3049021023741226 0.7893026378327245 0.8501687003620303 TTT	0.125804310135501 0.1265241360652981 0.097507376511985 TTT
0.0000000000000000	0.488371430340447 0.046511370988482 0.8304710714285690 FFF	
0.0000000000000000	0.6744182875655885 0.0203261227924081 0.8092800000000011 FFF	
Pt Co O H	0.3604656034782155 0.558139766911031 0.7880889285714261 FFF	Pt3Ni221-B 1.0000000000000000
13 3 1 1	0.7325580544776216 0.699767051482759 0.7457067857142832 FFF	5.4924200000000001 0.0000000000000000 0.0000000000000000
Selective dynamics	0.4186038210983104 0.3255818078418358 0.7245157142857153 FFF	0.0000000000000000 0.23863000000006 0.0000000000000000
Direct	0.6046504100686434 0.5813954519604607 0.0733246428571402 FFF	0.0000000000000000 25.0000000000000000
0.987098309852799 0.099016651640378 0.0049614717756180 TTT	0.1744190145078264 0.0203261227924081 0.8092800000000011 FFF	Pt Ni O H 1.0000000000000000
0.484182831851493 0.9971061524063116 0.9999881821265901 TTT	0.86046513063116 0.558139766911031 0.7880889285714261 FFF	26 6 1 1
0.2420937332516573 0.4905645409328707 0.0001403991244622 TTT	0.0465115472425890 0.839534110296580 0.768897857142852 FFF	Selective dynamics
0.7365397544551120 0.500592168798065 0.000848430474201 TTT	0.2325587814188594 0.069767051482759 0.7457067857142832 FFF	Direct
0.755499861897610 0.1587248254642469 0.90991679439702 TTT	0.7096977081774948 0.837209069709768 0.6821335714285712 FFF	-0.0014539763904782 -0.0093764501087606 -0.0005577854200792 TTT
0.49706565712967980 0.6599724886498671 0.9077364580726905 TTT	0.2906982711861588 0.83720906960709786 0.682133571428572 FFF	0.2492346031933195 0.717764322757550 0.9766505793643502 TTT
0.00124423570408 0.66949524505005 0.9087466695529947 TTT	0.4303572091457675 0.287617300222056 0.8934756371241172 TTT	-0.0029058139735611 0.4466834159663639 0.956287099946605 TTT
0.0000000000000000 0.333333032831228 0.8202884000000035 FFF	0.6133330935057911 0.5131352170689397 0.8740364535212830 TTT	0.250603554874563 0.1764382537736403 0.9284433727446041 TTT
0.499998182647545 0.3333334032831228 0.820288400000035 FFF	0.5465100203013441 0.8139534110296580 0.768897857142852 FFF	0.0000000000000000 0.222226268202334 0.7410848000000030 FFF
0.2499999091323772 0.83333313132487 0.820288400000035 FFF	0.9883721574752897 0.046511370988482 0.8304710714285690 FFF	0.249578179843519 0.062765763139795 0.8189205778984129 TTT
0.0000000000000000 0.703430239999964 FFF	0.1806454803995393 0.2355818078418358 0.724515714285713 FFF	0.499208375960962 -0.0087497913714262 -0.00128951586209917 TTT
0.499998182647545 0.0000000000000000 0.703430239999964 FFF	0.104651109098844 0.813954519604607 0.0733246428571402 FFF	0.74725580101365 0.193616106842007 0.9777261935361628 TTT
0.7499997727931317 0.5000002098493650 0.820288400000035 FFF	0.0518497114903108 -0.0080621128535907 0.0689959601024357 TTT	0.496341388210665 0.4531991898071083 0.949953210232386 TTT
0.247889727002222 0.1686197363876648 0.9099165688646309 TTT	0.9841749018014783 0.9045066978336948 0.709622656472414 TTT	0.749333421557987 0.175256502052480 0.9254956299614789 TTT
0.7499997727931317 0.83333313132487 0.820288400000035 FFF	0.051941750724890 0.8930860326220313 0.9395842782606996 TTT	0.502676057045816 0.16697387876566 TTT
0.2499999091323772 0.5000002098493650 0.820288400000035 FFF	0.754711611648590 0.6113961610846099 0.8443815448826014 TTT	0.5062665624154181 0.3366176198446099 0.8443815448826014 TTT
0.0237607056587160 0.976172868742487 0.08473315441319829 TTT	0.0876371830826461 0.157170236604442 0.0969095512160482 TTT	0.0876371830826461 0.157170236604442 0.0969095512160482 TTT
Pt3Co533-B	1.0000000000000000	5.5025079999999997 0.0000000000000000 0.0000000000000000
1.0000000000000000	1.3756269999999999 0.9205900000000003 0.0000000000000000	0.0000000000000000 28.0000000000000000
5.5025079999999997 0.0205900000000003 0.0000000000000000	0.0000000000000000 0.0000000000000000 0.0000000000000000	0.0000000000000000 0.777773731797666 0.792867999999986 FFF
1.3756269999999999 0.0000000000000000 0.0000000000000000	0.0000000000000000 0.0000000000000000 0.0000000000000000	0.249990896544659 0.944446467434489 0.7151935999999965 FFF
Pt Co O H	0.00342468979563 0.006783566093321 -0.001244293200892 TTT	0.00320984949764 0.339025750185684 0.8464630589541389 TTT
26 6 1 1	0.1844089210178864 0.266768625215860 0.8395214872154100 TTT	0.5000000000000000 0.5000000000000000 0.5000000000000000
Selective dynamics	0.870578183070951 0.512754783037433 0.959829823482242 TTT	0.749990896544659 0.944446467434489 0.7151935999999965 FFF
Direct	0.0597918131614949 0.748654387844753 0.939388784564757 TTT	0.5000000000000000 0.222226268202334 0.741084800000030 FFF
0.016189771335012 0.0095513819613773 0.997209384209322 TTT	0.936381172957900 0.275978983348814 0.8935495265402095 TTT	0.0000000000000000 0.111107065130952 0.637518800000023 FFF
0.193002359938187 0.2607650175599205 0.978215433953648 TTT	0.1165735252225083 0.5357682009711998 0.869644404644018 TTT	0.250567982127567 0.6136346529149634 0.8717440799596059 TTT
0.877718730182243 0.1515918493892104 0.8502442669832858 TTT	0.94197758817211372111 0.005141202838960 TTT	0.7515966525361276 0.059786916539608 0.815698231016684 TTT
0.0639117248314801 0.76583098736196 0.9429847029931686 TTT	0.685053322578126 0.26105091978964 0.813953913448213 TTT	0.749990896544659 0.944446467434489 0.7151935999999965 FFF
0.2445189180780833 0.0322032070464414 0.911975317053686 TTT	0.373589180390397 0.5135684704854024 0.958353913637964 TTT	0.5592708286725979 0.765456482544524 0.7293870158078 TTT
0.92346142472951 0.282377265333375 0.8922967007205519 TTT	0.5592708286725979 0.765456482544524 0.7293870158078 TTT	0.749990896544659 0.944446467434489 0.7151935999999965 FFF
0.110418413951846 0.353249681145210 0.8740943084735 TTT	0.748080310947243 0.033567694937429 0.123380732045246 TTT	0.249990896544659 0.38888686589879 0.6364103999999965 FFF
0.8006910370650145 0.171185538 0.8502442669832858 TTT	0.424644645419523 0.278220598564587 0.8397886371912764 TTT	0.249990896544659 0.33333940230537 0.6116275999999985 FFF
0.50119580235665622 0.0094923734381128 0.981257970387735 TTT	0.6155367050857014 0.5424087172130223 0.817029479290858 TTT	0.0007611062412696 0.378904645548323 0.0338398242072117 TTT
0.6864563235043566 0.260617402142131 0.956977898561455 TTT	0.300099477259947698 0.792312384491 0.956977898561455 TTT	0.013537706979432 0.478242711210937 0.0551369745663537 TTT
0.3825816240933488 0.509392514021431 0.956977898561455 TTT	0.488371430340447 0.046511370988482 0.8304710714285690 FFF	
0.561871362355278 0.7658698165895126 0.9381331302115300 TTT	0.6744182875655885 0.0323261227924081 0.8092800000000011 FFF	
0.74574083210983014 0.3255818078418358 0.7245157142832 FFF	0.5465100203013441 0.8139534110296580 0.768897857142832 FFF	Pt3Ni221-S 1.0000000000000000
0.304709892272783 0.78754302027052 0.8502442669832858 TTT	0.4186038210983104 0.3255818078418358 0.7245157142832 FFF	5.4924200000000001 0.0000000000000000 0.0000000000000000
0.4883714305340447 0.046511370988482 0.8304710714285690 FFF	0.6046504100686434 0.5813954519604607 0.0733246428571402 FFF	0.0000000000000000 0.23863000000006 0.0000000000000000
0.67442878572127588 0.1686197363876648 0.9099165688646302 TTT	0.9883721574752897 0.046511370988482 0.8304710714285690 FFF	0.0000000000000000 0.0000000000000000 0.0000000000000000
0.3604650634781755 0.558139766911031 0.7880889285714261 FFF	0.860465130663116 0.558139766911031 0.7880889285714261 FFF	Pt Ni O H 1.0000000000000000
0.7325580544776211 0.069767051482759 0.7457067857142832 FFF	0.0465115472425890 0.83720906960709786 0.682133571428572 FFF	26 6 1 1
0.0000000000000000 0.703430239999964 FFF	0.2325587814188594 0.069767051482759 0.7457067857142832 FFF	Selective dynamics
Pt Co O H	0.00342468979563 0.006783566093321 -0.001244293200892 TTT	0.00320984949764 0.339025750185684 0.8464630589541389 TTT
26 6 1 1	0.1046511370650145 0.171185538 0.8502442669832858 TTT	0.5000000000000000 0.5000000000000000 0.5000000000000000
0.61499778074139 0.531043724770381 0.8748114646021204 TTT	0.2906982711861588 0.83720906960709786 0.682133571428572 FFF	0.00076108728961901 0.29420827726027565 0.1565724067036700 TTT
0.5465100203013441 0.8139534110296580 0.768897857142832 FFF	0.424644645419523 0.278220598564587 0.8397886371912764 TTT	0.00076108728961901 0.29420827726027565 0.1565724067036700 TTT
0.2325587814188594 0.069767051482759 0.7457067857142832 FFF	0.300099477259947698 0.792312384491 0.956977898561455 TTT	0.12040016183151781 0.400783260795890 0.0596869547108262 TTT
0.91860480483059393 0.3255818078418358 0.7245157142832 FFF	0.2325587814188594 0.069767051482759 0.7457067857142832 FFF	0.75480388964477984 0.1770320705183 0.9250239829014587 TTT
0.1046511370088844 0.531043724770381 0.8748114646021204 TTT	0.1046511370088844 0.531043724770381 0.8748114646021204 TTT	0.50099655153199 0.8910045243596673 0.8925672714591866 TTT
0.61499778074139 0.531043724770381 0.8748114646021204 TTT	0.2906982711861588 0.83720906960709786 0.682133571428572 FFF	0.5030837044017549 0.958281516868572 0.997587113023327 TTT
0.5465100203013441 0.8139534110296580 0.768897857142832 FFF	0.170108728961901 0.29420827726027565 0.1565724067036700 TTT	0.75496866908605363 0.715110742720339 0.973662804334486 TTT
0.9883721574752897 0.046511370988482 0.8304710714285690 FFF	0.12040016183151781 0.400783260795890 0.0596869547108262 TTT	0.5018860349586563 0.4449422711047 0.9575049799049 TTT
0.91860480483059393 0.3255818078418358 0.7245157142832 FFF	0.5465100203013441 0.8139534110296580 0.768897857142832 FFF	0.75480388964477984 0.1770320705183 0.9250239829014587 TTT
0.1046511370088844 0.531043724770381 0.8748114646021204 TTT	0.1046511370088844 0.531043724770381 0.8748114646021204 TTT	0.50099655153199 0.8910045243596673 0.8925672714591866 TTT
0.8226778078072015 0.56869082210716 0.032626947129462 TTT	0.2906982711861588 0.83720906960709786 0.682133571428572 FFF	

Pt3Ni221-T			
1.0000000000000000	0.9894929169498647 0.0037334818203267 0.9990998026740134 T T T	0.7500000000000000 0.833334360041871 0.8163363999999973 F F F	
5.4924200000000001	0.1811331536339837 0.2644002518212030 0.9791097979015229 T T T	0.0000000000000000 0.724504799999983 F F F	
0.0000000000000000	0.869586153443416 0.514687606556102 0.9617685074837320 T T T	0.5000000000000000 0.724504799999983 F F F	
0.0000000000000000	0.0581212592725314 0.7678270092657816 0.940176020415246 T T T	0.2500000000000000 0.724504799999983 F F F	
Pt Ni O H	0.9326759973234026 0.2802122895337094 0.8926854284582354 T T T	0.7500000000000000 0.724504799999983 F F F	
26 6 1 1	0.1151995463779798 0.53914798843 0.8710229904273612 T T T	0.7572797452645035 0.1672908048110181 0.905836827203580 T T T	
Selective dynamics	0.4880273370830747 0.0104065911103013 0.94514647788740 T T T	0.4957739780563453 0.6663308720176828 0.9042174590500667 T T T	
Direct	0.6809916928271460 0.2650176047278141 0.9310360933674175 T T T	0.0031589406385597 0.6751873764994228 0.9061248578982728 T T T	
0.0016342227440943	0.3983707644928287 0.9930083367720768 T T T	0.2493424545034840 0.1668342606316893 0.9048764477184622 T T T	
0.2527365299833697	0.3703454916753930 0.9798217235162900 T T T	0.0063507818363069 0.0045597419223388 0.0785838047107253 T T T	
0.000503382701693	0.4374264374794420 0.94960177422658 T T T	0.1256596029787057 0.139707781727487 0.089517646320151 T T T	
0.249650946744328	0.16982582303910 0.9241668337684752 T T T		
0.0000000000000000	0.222222662802334 0.89248408000030 F F F		
0.2467216049084839	0.01631792244635238 0.8715851018463879 T T T	0.614896321160688 0.5439806656411134 0.871985795664132 T T T	0.1000000000000000
0.2482774471832245	0.0566337341145320 0.81732979752867840 T T T	0.3011865359731476 0.9337106528838 0.852205424291191 T T T	5.6235200000000001 0.0000000000000000 0.0000000000000000
0.50406498838762	0.9845346942630391 0.9969088781892533 T T T	0.04883723606853181 0.046511302471957 0.8307821248571458 F F F	0.0000000000000000 4.8701100000000004 0.0000000000000000
0.754646286182709	0.7104585367953530 0.9736959070255173 T T T	0.6744181072836710 0.302342131980508 0.8096456699999985 F F F	0.0000000000000000 25.0000000000000000
0.5043186758068042	0.439171191370902 0.95184886900918 T T T	0.10465112254130505 0.81395367950095 0.767325357142859 F F F	
0.752840881706202	0.1692158244156364 0.89248408000030 F F F	0.546511745273764 0.81395367950095 0.767325357142859 F F F	14 2 1 1
0.4978702165497328	0.888774051974122 0.89321894307542 T T T	0.41860488770766249 0.3255813385268524 0.7250210714285714 F F F	Selective dynamics
0.7498140159399399	0.6100511111922367 0.8684512068513841 T T T	0.60465110740822227 0.5813194945876584 0.7036865714285270 F F F	Direct
0.7495131649020175	0.0565470222351386 0.817239752867840 T T T	0.9883721786161459 0.046511302471957 0.8307821248571458 F F F	-0.0078797960705622 0.0122393949385507 -0.00358628994580297 T T T
0.498013353871633	0.329646469469710391 0.843489901194168 T T T	0.8604658165898513 0.558139849874695 0.7887477499999991 F F F	0.4914682062723983 0.006714562032081 -0.009778877723861 T T T
0.0000000000000000	0.77777737197666 0.79287699999986 F F F	0.046515112254130505 0.81394945876584 0.7036865714285270 F F F	0.2455872056598647 0.5074216484275216 -0.010465569373005 T T T
0.2499990896544659	0.499999931029820 0.7669763399999972 F F F	0.232557097865501 0.60976590513724 0.74617321428571416 F F F	0.7438102289337598 0.0102188594099387 -0.010405438776262 T T T
0.7499990896544659	0.499999931029820 0.7669763399999972 F F F	0.9180646950074527 0.3255813385268524 0.7250210714285714 F F F	0.0000000000000000 0.3333333333333357 0.8163363999999973 F F F
0.2499990896544659	0.499999931029820 0.7669763399999972 F F F	0.7906968160339460 0.8327087754031724 0.762162475714318 F F F	0.5000000000000000 0.3333333333333357 0.8163363999999973 F F F
0.2499990896544659	0.94444467443449 0.7151395399999992 F F F	0.246269116027052 0.20449272418117 0.914739283775910 T T T	0.2500000000000000 0.8333343600041871 0.8163363999999973 F F F
0.7499990896544659	0.94444467443449 0.7151395399999992 F F F	0.8025557617587586 0.7911609409239540 0.8514902131064847 T T T	0.7500000000000000 0.8333343600041871 0.8163363999999973 F F F
0.5000000000000000	0.6666666666666664 0.6893019999999979 F F F	0.732557491855273 0.66976590513724 0.767216115267116 F F F	0.0000000000000000 0.0000000000000000 0.7245047999999983 F F F
0.2499990896544659	0.3888886865898797 0.663410399999965 F F F	0.17441719251144889 0.3023251319850787 0.809629999999985 F F F	0.5000000000000000 0.0000000000000000 0.7245047999999983 F F F
0.7499990896544659	0.3888886865898797 0.663410399999965 F F F	0.290696720113963 0.8372087754031724 0.6827164285714318 F F F	0.2500000000000000 0.50000010266708586 0.7245047999999983 F F F
0.2499990896544659	0.8333339402230537 0.616127599999985 F F F	0.3604644179673017 0.558139849874695 0.7887477499999991 F F F	0.7694110466481262 0.1631903566567320 0.904443857382964 T T T
0.7499990896544659	0.8333339402230537 0.637518800000023 F F F	0.00977449358310 0.9816139049676018 0.0672161136033935 T T T	0.4940059859658686 0.66657549802448 0.9022737486430812 T T T
0.5000000000000000	0.1111107065130952 0.637518800000023 F F F	0.0040971780184685 0.91067051609651 0.081542899999972 F F F	0.0013151098482580 0.6733198310880342 0.9040323502706289 T T T
-0.0000000000000000	0.7777737197666 0.79287699999986 F F F	0.24831935453299 0.164082245722653 0.9036867211301594 T T T	
0.00029317634258	0.8883251217142111 0.8940587868817507 T T T	1.0000000000000000 0.0000000000000000 0.0000000000000000	
0.5000000000000000	0.222222662802334 0.741084800000030 F F F	5.4924179999999998 0.0000000000000000 0.0000000000000000	
0.0000000000000000	0.6666666666666664 0.6893019999999979 F F F	1.3731040000000001 0.9040479999999992 0.0000000000000000	
0.0000000000000000	0.1111107065130952 0.637518800000023 F F F	0.0000000000000000 0.0000000000000000 28.0000000000000000	
0.2441181130215777 0.683172517467012 0.0599981739925257 T T T	Pt3Ni53-T	Pt Cu O H	
0.3942071529374064 0.6259535219299111 0.0696854473284823 T T T	26 6 1 1	1.0000000000000000 0.0000000000000000 0.0000000000000000	
Pt3Ni53-B		Selective dynamics	
1.0000000000000000	0.0033745371690245 0.006410763701772 0.994576896421036 T T T	0.0000000000000000 0.0000000000000000 0.0000000000000000	
5.4924217999999998	0.1840595330053328 0.2670984534109688 0.98412390812073186 T T T	Pt Cu O	
1.3731040000000001	0.0404799999999992 0.0000000000000000 0.0000000000000000	13 3 1	
0.0000000000000000	0.0000000000000000 0.0000000000000000 0.0000000000000000	Selective dynamics	
Pt Ni O H	0.058017617519334 0.765132612022431 0.9398695827053523 T T T	Direct	
0.9361432932421792 0.2774214422881413 0.89417937431513 T T T	-0.0014307161038376 -0.012662944502640 -0.0065294673273318 T T T		
1.169342593824450 0.05360938621996171 0.7086977884759957 T T T	0.49769491516200 0.001487504382841 -0.0147466566566262 T T T		
0.4956505860634561	0.0070429412419178 0.9448040175082121 T T T	0.2541709257757800 0.4959608286410526 -0.0136693565123857 T T T	
0.6848928082374764	0.26225340731766897 0.8730865176153083 T T T	0.7443439428251465 0.495030778944369 -0.012948687942854 T T T	
0.3737444217302366 0.514733994242045 0.951096308218828 T T T	0.0000000000000000 0.3333333333333357 0.8163363999999973 F F F		
0.559817642210155 0.766121305698262 0.9402425002118836 T T T	0.5000000000000000 0.3333333333333357 0.8163363999999973 F F F		
0.74699981606432452 0.0417262881413 0.9125021719062000 T T T	0.2500000000000000 0.3333343600041871 0.8163363999999973 F F F		
0.0575912945065599	0.57670727972516302 0.938904028134370 T T T	0.424675385438482 0.27451432056897 0.8730865174285712 F F F	
0.934515152184415	0.2781904312871902 0.8926803802161515 T T T	0.616167500532150 0.541909060329971 0.87187392721855 T T T	
0.117957346251810	0.3563971023957711 0.87151973992273 T T T	0.300837267712912 0.91695768947364364 0.8519312378366936 T T T	
0.4968041218296506	0.07409317494559 0.953353746668607 T T T	0.488372360853181 0.046511302471957 0.8307821248571458 F F F	
0.688037262638110	0.26119170731571 0.8372087875203724 T T T	0.6744181072836710 0.3023251319850786 0.809629999999985 F F F	
0.3736086286963765	0.5176114261306997 0.964760507318914 T T T	0.1046512254130505 0.58139495876584 0.7080629999999973 F F F	
0.50656450491916	0.76764103717193 0.9396486864247 T T T	0.546511745257364 0.3255813385268524 0.7250210714285712 F F F	
0.7463463706339396	0.16668480968816 0.91250581560730878 T T T	0.4180646477967062249 0.3255813385268524 0.7250210714285712 F F F	
0.4284642353302444	0.278262317493053 0.893751604323244 T T T	0.60465140725220 0.58139495876584 0.7038685174285720 F F F	
0.612500520624411	0.5418915193861387 0.8732629132851 T T T	0.9883721786161459 0.5581398495746879 0.7088747499999991 F F F	
0.301050457449133	0.791643077291278 0.889337578364928 T T T	0.4065115163182043 0.813953679500959 0.767325357142859 F F F	
0.488372360685318	0.046511302149557 0.830780721428571458 F F F	0.0465115163182043 0.813953679500959 0.767325357142859 F F F	
0.67444718721786161459	0.046511302149557 0.830780721428571458 F F F	0.323557097865501 0.699765905013724 0.7461732142857116 F F F	
0.1046512254130505	0.58139495716584 0.7038685176153082 F F F	0.9180646950074527 0.3255813385268524 0.7250210714285712 F F F	
0.546511745257364	0.813953679500959 0.767325357142859 F F F	0.7096896160339460 0.837207754031724 0.6827164285714318 F F F	
0.4186477076249	0.3255813385268524 0.7250210714285712 F F F	0.24543159064383354 0.0192473203055492 0.9139151371473342 F F F	
0.604651407422227	0.581398499874695 0.7884774999999991 F F F	0.80417389107197 0.787634637431189 0.8509701204286999 T T T	
0.9883721786161459	0.046511302149557 0.830780721428571458 F F F	0.732557491857223 0.69976590513724 0.87187392721855 F F F	
0.860465168508513	0.5581398499874695 0.7884774999999991 F F F	0.1744179251244988 0.203251319850786 0.8096299999999985 F F F	
0.046511516338204	0.813953679500959 0.767325357142859 F F F	0.2906965710370317 0.837207754031724 0.6827164285714318 F F F	
0.232			

s-Pt221-8			
1.000000000000000			
5.4924200000000001	0.000000000000000	0.000000000000000	0.000000000000000
0.000000000000000	8.238630000000000	0.000000000000006	25.0000000000000
Pt O H			
32 1 1			
Selective dynamics			
Direct			
-0.000000000000000	0.996007359244662	0.0080608359566362	7 T T
0.250573000000000	0.000000000000000	0.000000000000000	0.000000000000000
0.000000000000000	0.000000000000000	0.000000000000000	0.000000000000000
Pt O H			
32 1 1			
Selective dynamics			
Direct			
-0.000000000000000	0.996007359244662	0.0080608359566362	7 T T
0.248325399118873	0.6131290685064498	0.8763425474450729	7 T T
0.2494817947497244	0.0608611943598981	0.82160644584821	7 T T
0.500000000000000	0.000000000000000	0.9967892216858743	0.006588626352984
0.7494287989296970	0.7241857285014106	0.985049197550599	7 T T
0.500000000000000	0.000000000000000	0.454848954857357	0.959676968083671
0.74952897701235	0.1789445747947493	0.9346989149416431	7 T T
0.500000000000000	0.000000000000000	0.22222629999974	0.1784080000030 F F
0.248325399118873	0.6131290685064498	0.8763425474450729	7 T T
0.2494817947497244	0.0608611943598981	0.82160644584821	7 T T
0.500000000000000	0.000000000000000	0.3358972998116458	0.058505015850227
0.7494287989296970	0.7241857285014106	0.985049197550599	7 T T
0.500000000000000	0.000000000000000	0.454848954857357	0.959676968083671
0.74952897701235	0.1789445747947493	0.9346989149416431	7 T T
0.500000000000000	0.000000000000000	0.000000000000000	0.000000000000000
0.5465117452573764	0.81395367950095	0.6757351743859 F F	
0.7516728403881113	0.6131290685064498	0.8763425474450729	7 T T
0.7505163852502814	0.0608611943598981	0.82160644584821	7 T T
0.500000000000000	0.000000000000000	0.3358972998116458	0.058505015850227
0.7494287989296970	0.7241857285014106	0.985049197550599	7 T T
0.500000000000000	0.000000000000000	0.454848954857357	0.959676968083671
0.74952897701235	0.1789445747947493	0.9346989149416431	7 T T
0.500000000000000	0.000000000000000	0.000000000000000	0.000000000000000
0.5465117452573764	0.81395367950095	0.6757351743859 F F	
0.7505163852502814	0.0608611943598981	0.82160644584821	7 T T
0.500000000000000	0.000000000000000	0.3358972998116458	0.058505015850227
0.7494287989296970	0.7241857285014106	0.985049197550599	7 T T
0.500000000000000	0.000000000000000	0.454848954857357	0.959676968083671
0.74952897701235	0.1789445747947493	0.9346989149416431	7 T T
0.500000000000000	0.000000000000000	0.000000000000000	0.000000000000000
0.5465117452573764	0.81395367950095	0.6757351743859 F F	
0.749499909000000	0.499999389999999	0.7669763399999972	F F
0.749999090000000	0.499999389999999	0.7669763399999972	F F
0.249999090000000	0.494444650000000	0.7151395399999992	F F
0.749999090000000	0.494444650000000	0.7151395399999992	F F
0.500000000000000	0.000000000000000	0.6666666666666666	0.6893019999999979
0.249999090000000	0.388886600000000	0.6343013099999965	F F
0.749999090000000	0.388886600000000	0.6343013099999965	F F
0.500000000000000	0.000000000000000	0.3353271909770110	0.8522080850209446
0.500000000000000	0.000000000000000	0.77777730000026	0.7392876999999966
0.249999090000000	0.896458341857815	0.9009163143594561	7 T T
0.500000000000000	0.000000000000000	0.22222629999974	0.74108400000030 F F
0.249999090000000	0.29 0.833339400000000	0.81627058779999998	F F
0.749999090000000	0.29 0.833339400000000	0.81627058779999998	F F
0.500000000000000	0.000000000000000	0.1111107099999984	0.6375188000000023
0.249999090000000	0.000000000000000	0.3353271909770110	0.8522080850209446
0.500000000000000	0.000000000000000	0.77777730000026	0.7392876999999966
0.249999090000000	0.896458341857815	0.9009163143594561	7 T T
0.500000000000000	0.000000000000000	0.22222629999974	0.74108400000030 F F
0.249999090000000	0.000000000000000	0.6666666666666666	0.6893019999999979
0.749999090000000	0.000000000000000	0.6375188000000023	F F
0.249999090000000	0.363262781423041	0.0414942851985863	7 T T
0.249999090000000	0.000000000000000	0.45696303447985636	0.0655751110908987
s-Pt221-SE			
1.000000000000000			
5.4924200000000001	0.000000000000000	0.000000000000000	0.000000000000000
0.000000000000000	8.238630000000000	0.000000000000006	25.0000000000000
Pt O H			
32 1 1			
Selective dynamics			
Direct			
-0.000000000000000	0.995332516148934	0.004081746968354	0.002849496054146
0.1848008199178049	0.257723040835128	0.986037039338534	7 T T
0.873320984179230	0.507659724752704	0.9682747079856555	T T T
0.060370208863622	0.576404409036262	0.945086130665309	T T T
0.25117524997423	0.0157396507995999997	0.92720107142857110	F T T
0.000000000000000	0.23222629999974	0.823670708136793	0.6827164285714318
0.248638018294611	0.000000000000000	0.823670708136793	0.6827164285714318
0.749999090000000	0.000000000000000	0.33592303264909	0.823670708136793
0.249999090000000	0.000000000000000	0.8955274381067867	0.823670708136793
0.749999090000000	0.000000000000000	0.1111107099999984	0.6375188000000023
0.249999090000000	0.000000000000000	0.363262781423041	0.0414942851985863
0.249999090000000	0.000000000000000	0.45696303447985636	0.0655751110908987
s-Pt221-5E			
1.000000000000000			
5.4924200000000001	0.000000000000000	0.000000000000000	0.000000000000000
0.000000000000000	8.238630000000000	0.000000000000006	25.0000000000000
Pt O H			
32 1 1			
Selective dynamics			
Direct			
-0.000000000000000	0.995332516148934	0.004081746968354	0.002849496054146
0.1848008199178049	0.257723040835128	0.986037039338534	7 T T
0.873320984179230	0.507659724752704	0.9682747079856555	T T T
0.060370208863622	0.576404409036262	0.945086130665309	T T T
0.25117524997423	0.0157396507995999997	0.92720107142857110	F T T
0.000000000000000	0.23222629999974	0.823670708136793	0.6827164285714318
0.248638018294611	0.000000000000000	0.823670708136793	0.6827164285714318
0.749999090000000	0.000000000000000	0.33592303264909	0.823670708136793
0.249999090000000	0.000000000000000	0.8955274381067867	0.823670708136793
0.749999090000000	0.000000000000000	0.1111107065130952	0.6375188000000023
0.249999090000000	0.000000000000000	0.363262781423041	0.0414942851985863
0.249999090000000	0.000000000000000	0.45696303447985636	0.0655751110908987
s-Pt3T111			
1.000000000000000			
5.494999089644659	0.000000000000000	0.000000000000000	0.000000000000000
0.000000000000000	8.238863000000000	0.000000000000000	0.000000000000000
Pt O H			
32 1 1			
Selective dynamics			
Direct			
-0.00055818109314985	-0.0045284808757919	0.0012484155174684	T T T
0.4922098726137485	0.0018385918733378	-0.001970142250916	T T T
0.0015662070690757	0.49256838135492	-0.002014951712443	T T T
0.4989274510747866	0.4994305970114449	0.001759211813489	T T T
0.6760705478378546	0.1657501803403921	0.90705668486169	T T T
0.20969972011363	0.837208775407813	0.6827164285714318	F F F
0.749999089644659	0.000000000000000	0.6363751880000000	0.000000000000000
0.000000000000000	0.6634301309999965	0.6893019999999979	F F F
0.249999089644659	0.000000000000000	0.33592303264909	0.823670708136793
0.249999089644659	0.000000000000000	0.8955274381067867	0.823670708136793
0.749999089644659	0.000000000000000	0.1111107065130952	0.6375188000000023
0.249999089644659	0.000000000000000	0.363262781423041	0.0414942851985863
0.249999089644659	0.000000000000000	0.45696303447985636	0.0655751110908987
Pt Ti O H			
32 1 1			
Selective dynamics			
Direct			
-0.00055818109314985	-0.0045284808757919	0.0012484155174684	T F F
0.4922098726137485	0.0018385918733378	-0.001970142250916	F F F
0.0015662070690757	0.49256838135492	-0.002014951712443	F F F
0.4989274510747866	0.4994305970114449	0.001759211813489	F F F
0.6760705478378546	0.1657501803403921	0.90705668486169	F F F
0.20969972011363	0.837208775407813	0.6827164285714318	F F F
0.749999089644659	0.000000000000000	0.6363751880000000	0.000000000000000
0.000000000000000	0.6634301309999965	0.6893019999999979	F F F
0.249999089644659	0.000000000000000	0.33592303264909	0.823670708136793
0.249999089644659	0.000000000000000	0.8955274381067867	0.823670708136793
0.749999089644659	0.000000000000000	0.1111107065130952	0.6375188000000023
0.249999089644659	0.000000000000000	0.363262781423041	0.0414942851985863
0.249999089644659	0.000000000000000	0.45696303447985636	0.0655751110908987
Pt Ti O H			
32 1 1			
Selective dynamics			
Direct			
-0.00055818109314985	-0.0045284808757919	0.0012484155174684	T F F
0.4922098726137485	0.0018385918733378	-0.001970142250916	F F F
0.0015662070690757	0.49		

0.36046433 0.55813963 0.78492821 F F F  
0.08070246 0.97080480 0.06747963 T T T  
0.0399648 0.05854370 0.08670678 T T T

Pt3Ti53-T  
1.000000000000000  
5.58475999999996 0.0000000000000000 0.0000000000000000  
1.3961450000000000 9.1551320000000000 0.0000000000000000  
0.0000000000000000 0.0000000000000000 28.000000000000000  
Pt Ti O H  
26 6 1  
Selective dynamics  
Direct  
0.003678577700862 0.010400128736886 0.993920446353891 T T T  
0.187507419130016 0.26692775794812442 0.9811334052810819 T T T  
0.8734461255669316 0.0588307579381356 0.957440042613145 T T T  
0.0587808342747676 0.7608155626909531 0.9379816113418696 T T T  
0.9370720696627721 0.2745259480068168 0.890925356330783 T T T  
0.1231747707261380 0.5326832925371532 0.8670581359896766 T T T  
0.4960772073544779 0.0117267727908934 0.9936810453878302 T T T  
0.6870160380668235 0.263437360584309 0.9797072154622957 T T T  
0.3779843363498383 0.5099749954637697 0.9554898446919138 T T T  
0.5574463388836574 0.7636377572110042 0.937737568522826 T T T  
0.7513864067410308 0.01045355452386 0.910892116358437 T T T  
0.4273179059163263 0.269231879555296 0.8921421626534541 T T T  
0.617959351133263 0.54477523751354 0.886860525441848 T T T  
0.298729268620196 0.7924805687702691 0.85050341689569521 T T T  
0.488372704637208 0.465116177461979 0.8279428571428582 F F F  
0.67444179673683764 0.302365722167 0.8767255122119892 F F F  
0.1046511774075682 0.5813954402842043 0.698899642857142146 F F F  
0.5465118134679230 0.8139535290152011 0.7634210714285743 F F F  
0.418604818856753 0.32558132233998 0.827942857142888 F F F  
0.6046513567121323 0.5813954402842043 0.6988996428571426 F F F  
0.9883720913991567 0.465116177451979 0.8279428571428582 F F F  
0.8604659374985104 0.5813953214111018 0.7849282142857135 F F F  
0.046511840353660 0.189535290152011 0.7634210714285743 F F F  
0.2325573313082216 0.6997674266193005 0.7419139285714280 F F F  
0.9186046397941112 0.325581322233998 0.7204067857142888 F F F  
0.790698485934649 0.8372093378883037 0.6773925000000034 F F F  
0.24347075311774996 0.027665053884478 0.9181363997414739 T T T  
0.8074009608438188 0.7831393634021325 0.8537606486420014 T T T  
0.7325575310377700 0.6697674266193005 0.7419139285714280 F F F  
0.1744177883040123 0.302325513502973 0.80643571428571119 F F F  
0.290698743124239 0.8372093378883037 0.6773925000000034 F F F  
0.3604643259174694 0.5813953214111018 0.7849282142857135 F F F  
0.1778158784888314 0.2754977926490105 0.0532775974796466 T T T  
0.0063933503640553 0.3010009649722210 0.061710428699034 T T T  
0.499996376614675 0.0000000000000000 0.7295912399999978 F F F

Pt3Cu11  
1.000000000000000  
5.5197000000000003 0.0000000000000000 0.0000000000000000  
2.7598500000000001 4.780199999999998 0.0000000000000000  
0.0000000000000000 0.0000000000000000 25.000000000000000  
Pt Cu O H  
13 3 1  
Selective dynamics  
Direct  
0.9942302511598793 0.9945497928811884 0.0039390441340718 T T T  
0.492627473688917 0.99672962330184 0.998122904320137 T T T  
0.99642862188342487 0.4929242346899471 0.99811789858159 T T T  
0.4952401052299357 0.4955633050213680 0.0021568447548430 T T T  
0.6719337922870877 0.164532354943765 0.9089438422890368 T T T  
0.164409469787826 0.6721624421761290 0.908536419195818 T T T  
0.6674394528160977 0.6675286335609033 0.907711040380393 T T T  
0.8333334379314650 0.333331241370630 0.819727479999974 F F F  
0.3333330755929325 0.333331241370630 0.819727479999974 F F F  
0.3333331036193934 0.333332704745317 0.819727479999974 F F F  
0.0000000000000000 0.0000000000000000 0.7295912399999978 F F F  
0.499996376614675 0.0000000000000000 0.7295912399999978 F F F

Pt3Cu53-S  
1.000000000000000  
5.51995999999997 0.0000000000000000 0.0000000000000000  
1.379923999999999 0.948766999999999 0.0000000000000000  
0.0000000000000000 0.0000000000000000 28.000000000000000  
Pt Cu O H  
26 6 1  
Selective dynamics  
Direct  
0.003678577700862 0.010400128736886 0.993920446353891 T T T  
0.187507419130016 0.26692775794812442 0.9811334052810819 T T T  
0.8734461255669316 0.0588307579381356 0.957440042613145 T T T  
0.0587808342747676 0.7608155626909531 0.9379816113418696 T T T  
0.9370720696627721 0.2745259480068168 0.890925356330783 T T T  
0.1231747707261380 0.5326832925371532 0.8670581359896766 T T T  
0.4960772073544779 0.0117267727908934 0.9936810453878302 T T T  
0.6870160380668235 0.263437360584309 0.979707215462220 T T T  
0.3779843363498383 0.5099749954637697 0.9554898446919138 T T T  
0.5574463388836574 0.7636377572110042 0.937737568522826 T T T  
0.7513864067410308 0.01045355452386 0.910892116358437 T T T  
0.4273179059163263 0.269231879555296 0.8921421626534541 T T T  
0.617959351133263 0.54477523751354 0.886860525441848 T T T  
0.298729268620196 0.7924805687702691 0.85050341689569521 T T T  
0.488372704637208 0.465116177461979 0.8279428571428582 F F F  
0.67444179673683764 0.302365722167 0.8767255122119892 F F F  
0.1046511774075682 0.5813954402842043 0.6988996428571426 F F F  
0.488372353037045 0.046511309203637 0.8299417857142828 F F F  
0.5465118134679230 0.8139535290152011 0.7634210714285743 F F F  
0.418604818856753 0.32558132233998 0.827942857142888 F F F  
0.6046513567121323 0.5813954402842043 0.6988996428571426 F F F  
0.9883720913991567 0.465116177451979 0.8279428571428582 F F F  
0.8604659374985104 0.5813953214111018 0.7849282142857135 F F F  
0.046511840353660 0.189535290152011 0.7634210714285743 F F F  
0.2325573313082216 0.6997674266193005 0.7419139285714280 F F F  
0.9186046397941112 0.325581322233998 0.7204067857142888 F F F  
0.790698485934649 0.8372093378883037 0.6773925000000034 F F F  
0.24347075311774996 0.027665053884478 0.9181363997414739 T T T  
0.8074009608438188 0.7831393634021325 0.8537606486420014 T T T  
0.7325575310377700 0.6697674266193005 0.7419139285714280 F F F  
0.1744177883040123 0.302325513502973 0.8064357142857119 F F F  
0.8064657744777864 0.581397995992177 0.78474271428571404 F F F  
0.0465115855010936 0.8139536579956115 0.766169642857142857 F F F  
0.2325573962244079 0.0697675136920124 0.8299417857142828 T T T  
0.11590769827391016427 0.5367007743301382 0.870097210616427 T T T  
0.495842527100892 0.03773259716574 0.994262373974694 T T T  
0.6832646748734006 0.2628167399369057 0.9800147069354630 T T T  
0.37213463615205 0.514673731570181 0.9571562849160982 T T T  
0.5602801036660604 0.667069847018363 0.9395892135487951 T T T  
0.7446748900241676 0.0166802049783108 0.9116616701280056 T T T  
0.42439269402435394 0.2751111228443343 0.8931508008194682 T T T  
0.6150131946286505 0.542913190628653 0.8707162718257118 T T T  
0.299652037845893 0.972533030267339 0.851276474017897 T T T  
0.4883723530337045 0.046511309203637 0.8299417857142828 F F F  
0.6744183457570117 0.302325167167575 0.8086842857142855 F F F  
0.1046512745880150 0.5813949016479256 0.702397857142857 F F F  
0.5465118134679230 0.8139536579956115 0.766169642857142852 F F F  
0.4186050186416921 0.3255813747884133 0.723553571428601 F F F  
0.6046516369268176 0.5813949016479256 0.702397857142857 F F F  
0.988372172694091 0.046511309203637 0.8299417857142828 F F F  
0.8604657744777864 0.581397995992177 0.78474271428571404 F F F  
0.0465115855010936 0.8139536579956115 0.7661696428571428601 F F F  
0.2325573962244079 0.0697675136920124 0.8299417857142828 T T T  
0.018604653028967 0.3255813747884133 0.723553571428601 F F F  
0.7325575785632033 0.0697675136920124 0.744912499999981 F F F  
0.1744179834182162 0.7690274042703990 0.9399920108648364 T T T  
0.9303592824092647 0.2815340585679423 0.8919374938755950 T T T  
0.1123607425429956 0.5401917829374804 0.87094273180476 T T T  
0.48751696166281298 0.0102793319446795 0.00611570608415 T T T  
0.6794359855829007 0.264347281850142 0.980162061788234 T T T  
0.3694610403234326 0.5140323392472866 0.9580393577026853 T T T  
0.5574033020887036 0.7664011835885149 0.9398805310352325 T T T

## S7. References

---

- 1 T. Rurigaki, A. Hitotsuyanagi, M. Nakamura, N. Sakai, N. Hoshi, *J. Electroanal. Chem.*, 2014, **716**, 58-62.
- 2 V. R. Stamenković, B. Fowler, B. S. Mun, G. Wang, P. N. Ross, C. A. Lucas, N. M. Marković, *Science*, 2007, **315**, 493-497.
- 3 S. Kobayashi, M. Wakisaka, D. A. Tryk, A. Iiyama, H. Uchida, *J. Phys. Chem. C*, 2017, **121**, 11234–11240.
- 4 Y. Takesue, M. Nakamura, N. Hoshi, *Phys. Chem. Chem. Phys.*, 2014, **16**, 13774.
- 5 V. Stamenković, T.J. Schmidt, P.N. Ross, N.M. Marković, *J. Electroanal. Chem.*, 2003, **554–555**, 191-199.
- 6 I. E. L. Stephens, A. S. Bondarenko, F. J. Perez-Alonso, F. Calle-Vallejo, L. Bech, T. P. Johansson, A. K. Jepsen, R. Frydendal, B. P. Knudsen, J. Rossmeisl, I. Chorkendorff, *J. Am. Chem. Soc.*, 2011, **133**, 5485–5491.
- 7 I. E. L. Stephens, A. S. Bondarenko, L. Bech, I. Chorkendorff, *ChemCatChem*, 2012, **4**, 341–349.
- 8 B. Garlyyev, M. D. Pohl, V. Čolić, Y. Liang, F. K. Butt, A. Holleitner, A. S. Bandarenka, *Electrochem. Commun.*, 2018, **88**, 10–14.
- 9 R. W. Haid, R. M. Kluge, Y. Liang, A. S. Bandarenka, *Small Methods*, 2020, **4**, 2000710.

- 
- 10 R. M. Kluge, E. Psaltis, R. W. Haid, S. Hou, T. O. Schmidt, O. Schneider, B. Garlyyev, F. Calle-Vallejo, A. S. Bandarenka, *ACS Appl. Mater. Interfaces*, 2022, **14**, 19604.
- 11 R. M. Kluge, R. W. Haid, A. S. Bandarenka, *J. Catal.*, 2021, **396**, 14-22.
- 12 Z.-D. He, S. Hanselman, Y.-X. Chen, M. T. M. Koper, F. Calle-Vallejo, *J. Phys. Chem. Lett.*, 2017, **8**, 2243–2246.
- 13 J. K. Nørskov, J. Rossmeisl, A. Logadottir, L. Lindqvist, J. R. Kitchin, T. Bligaard, H. Jónsson, *J. Phys. Chem. B*, 2004, **108**, 17886–17892.
- 14 E. Sargeant, F. Illas, P. Rodríguez, F. Calle-Vallejo, *J. Electroanal. Chem.*, 2021, **896**, 115178.
- 15 F. Calle-Vallejo, A. S. Bandarenka, *ChemSusChem*, 2018, **11**, 1824–1828.
- 16 R. Guidelli, R. G. Compton, J. M. Feliu, E. Gileadi, J. Lipkowski, W. Schmickler, S. Trasatti, *Pure Appl. Chem.*, 2014, **86**, 245–258.
- 17 F. Calle-Vallejo, M. D. Pohl, D. Reinisch, D. Loffreda, P. Sautet, A. S. Bandarenka, *Chem. Sci.*, 2017, **8**, 2283–2289.
- 18 A. Hitotsuyanagi, M. Nakamura, N. Hoshi, *Electroch. Acta*, 2012, **82**, 512-516.